

Lawrence Berkeley National Laboratory

Recent Work

Title

THEORETICAL ANALYSIS OF THE USE OF GERMANIUM DETECTORS FOR TIME-OF-FLIGHT EMISSION TOMOGRAPHY

Permalink

<https://escholarship.org/uc/item/5nt4s038>

Authors

Llacer, J.
Spieler, H.
Goulding, F.S.

Publication Date

1982-05-01

c.2



Lawrence Berkeley Laboratory

UNIVERSITY OF CALIFORNIA

RECEIVED
LAWRENCE
BERKELEY LABORATORY

AUG 2 1982

LIBRARY AND
DOCUMENTS SECTION

Engineering & Technical Services Division

Presented at the Symposium on Time-of-Flight Emission Tomography, St. Louis, MO, May 17-19, 1982; and to be published in the Proceedings

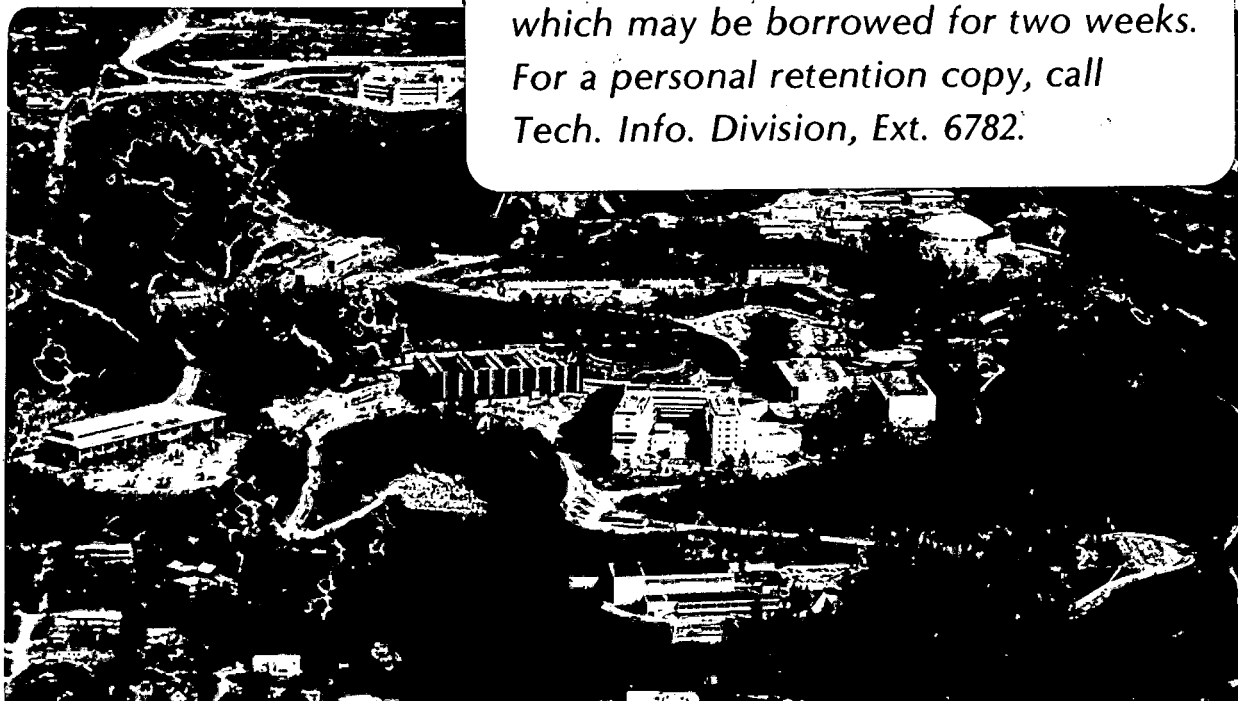
THEORETICAL ANALYSIS OF THE USE OF GERMANIUM DETECTORS FOR TIME-OF-FLIGHT EMISSION TOMOGRAPHY

Jorge Llacer, Helmuth Spieler and Frederick S. Goulding

May 1982

TWO-WEEK LOAN COPY

This is a Library Circulating Copy which may be borrowed for two weeks. For a personal retention copy, call Tech. Info. Division, Ext. 6782.



LBL-14401
c.2

DISCLAIMER

This document was prepared as an account of work sponsored by the United States Government. While this document is believed to contain correct information, neither the United States Government nor any agency thereof, nor the Regents of the University of California, nor any of their employees, makes any warranty, express or implied, or assumes any legal responsibility for the accuracy, completeness, or usefulness of any information, apparatus, product, or process disclosed, or represents that its use would not infringe privately owned rights. Reference herein to any specific commercial product, process, or service by its trade name, trademark, manufacturer, or otherwise, does not necessarily constitute or imply its endorsement, recommendation, or favoring by the United States Government or any agency thereof, or the Regents of the University of California. The views and opinions of authors expressed herein do not necessarily state or reflect those of the United States Government or any agency thereof or the Regents of the University of California.

THEORETICAL ANALYSIS OF THE USE OF GERMANIUM DETECTORS
FOR TIME-OF-FLIGHT EMISSION TOMOGRAPHY

Jorge Llacer, Helmuth Spieler and Frederick S. Goulding

Lawrence Berkeley Laboratory, University of California
Berkeley, California 94720 U.S.A.

ABSTRACT

A theoretical analysis of the timing capabilities of Ge semiconductor detectors in time-of-flight positron emission tomography is presented. The effect of detector size on efficiency and time resolution is discussed. The relevant noise sources are determined and the optimum filter is derived to optimize the slope-to-noise ratio, while minimizing the effect of collection time variations on time resolution. The performance of the ideal filter is compared with a single RC integrator. For a lower energy threshold of 200 keV, time resolution of better than 250 ps seems to be a realistic goal for a detector of 0.5 x 0.5 cm cross section and 3 cm length. This detector would yield an overall efficiency of 36% for 511 keV gamma-rays and 80% of the detected photons would fall in the Gaussian part of the timing spectrum.

INTRODUCTION

The use of germanium detectors for time-of-flight positron emission imaging was first proposed by Llacer and Cho in 1973¹. At that time the role of time-of-flight techniques in improving the signal to noise ratio of image reconstructions was not understood, and the idea was not pursued experimentally. In more recent papers Kaufman et al^{2,3} have discussed the potential of Ge detectors for time-of-flight assisted tomography and presented some preliminary data. Recent discussions with M. Ter-Pogossian and N. Mullani have stimulated our interest in reassessing the timing properties of Ge-detectors in the light of modern technology. In this paper we present a theoretical analysis which points out the relevant parameters in the detector and its associated electronics and shows their effect on timing accuracy. The purpose of this analysis is to define realistic goals and outline ways of achieving them. Practical aspects of timing with semiconductor detectors have been treated in a recent tutorial paper by Spieler⁴. Measurements to ascertain the limits of available components in this specific application will begin shortly.

Time resolution in a semiconductor detector system is determined by the detected energy, the size and shape of the detector, electronic noise

and the filtering of signal and noise components. These are treated individually in the following sections.

DETECTOR GEOMETRY

Size and shape of the detector affect both efficiency and collection time. The detection efficiency for 511 keV gamma-rays has been calculated for three crystal sizes which seem appropriate for this application. The length of the detectors is 3 cm in the direction of the incoming gamma-rays. The square cross sections have sides of 0.5, 0.75 and 1 cm. The calculation has been carried out by a Monte Carlo code written by S. E. Derenzo⁵, which has been validated in independent measurements. Table 1 shows the results of the calculation for five different energy thresholds--assuming perfect energy resolution. Uniform perpendicular illumination of the entrance face is assumed.

Table 1

Detection Efficiency of a Single Ge Detector for 511 keV Photons. The detector's length is 3 cm.

Energy Threshold (keV)	Side Dimension (cm)		
	0.5	0.75	1.0
100	52 %	52 %	52 %
200	36 %	38 %	39 %
300	16 %	19 %	22 %
400	6.4%	8.3%	10.3%
510	6.0%	7.8%	9.8%

Efficiency at lower energies is practically identical for the three sizes, whereas the efficiency at 510 keV increases by about 60% when the side dimension is increased from 0.5 to 1.0 cm.

SIGNAL GENERATION

The process of signal generation in a semiconductor detector will be reviewed briefly in order to demonstrate the origin of the waveforms from which the timing information must be derived. Consider a charge in a semiconductor depletion layer of thickness d , Fig. 1. We shall assume that the electric field in the depletion region is uniform and high enough ($> 10^3$ V/cm) that the electrons and holes generated by ionizing radiation move at a constant saturation velocity v_s . As a single carrier moves, the change in induced charge at each contact is $dq/dt = qv_s/d$. This current is constant during the transit time.

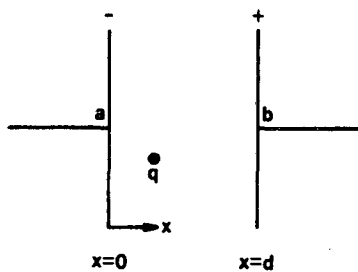


Fig. 1. A unit charge q at a distance x from contact a of a semiconductor detector of thickness d .

Depending on the position along x where a gamma-ray interaction occurs, the current pulses will have different shapes. At any time the current flow is due to the simultaneous movement of electrons and holes, or due to one of these if the other has been collected. Consider first a number of electron-hole pairs generated very near contact a in Fig. 1. The current i will be almost entirely due to the motion of electrons. The total collected charge Q will be given by

$$Q = \int_0^{\tau_t} i dt = \frac{q E_d}{\epsilon} \quad (1)$$

where $\tau_t = d/v_s$ is the transit time, E_d is the detected energy in eV, ϵ is the average energy needed to generate one electron hole pair (2.98 eV in Ge) and q is the electronic charge. This current pulse is shown in Fig. 2a. The transit time for a 1 cm thick detector is approximately 100 ns and decreases linearly with detector thickness.

Next, consider a gamma-ray interaction at $x = d/2$. Both electrons and holes will contribute to the current flow, but current will only flow during $\tau_t/2$ (Fig. 2b). Since the currents due to electrons and holes add, the instantaneous current is twice that of the first case. Examples

for interactions at $x = d/4$ and $d/16$ are shown in Figs. 2c and 2d, respectively.

There will be a large number of events where 511 keV gamma-rays will lead to more than one interaction in a Ge detector (Compton scattering followed by photoelectric absorption, for example). Figure 2e shows the current pulse for a hypothetical event in which two interactions occurred at $x = d/4$ and $d/2$, each depositing an energy $E_d/2$. This general class of event will be rather frequent: Derenzo's Monte Carlo code⁵ shows that for a 200 keV energy threshold and a detector with a side dimension of 1 cm, 48% of the detected particles have one single interaction, 29% undergo two interactions and the remaining 33% suffer three or more interactions.

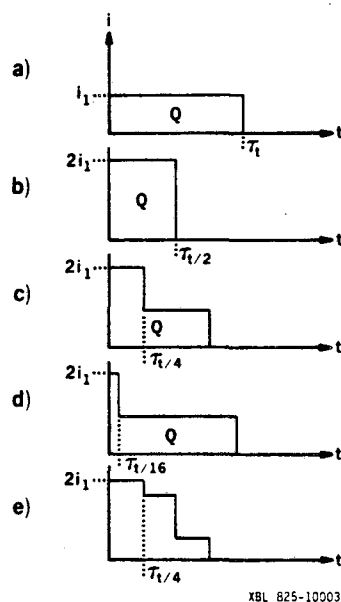


Fig. 2. Current pulse shapes in a semiconductor detector: a) For a detected event infinitesimally near one of the contacts, b) Single event occurring at $x = d/2$, c) Single event at $d/4$, d) Single event at $d/16$, e) Two events, each depositing $Q/2$, occurring at $d/4$ and $d/2$ respectively.

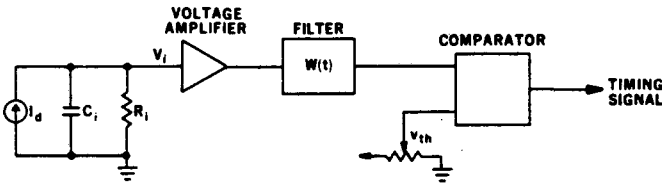
It is important to note that, except in the case of a single interaction arbitrarily close to one of the contacts, all current signals initially attain a current $2i_1$, where $i_1 = Q/\tau_t$; that is, nearly all signals begin with a dual carrier component of equal magnitude.

EQUIVALENT INPUT CIRCUIT

Signal

A simplified model of a detector input circuit is shown in Fig. 3. The detector is represented by a current source and a parallel capacitance,

which is lumped together with the input capacitance of the amplifier to form the total input capacitance, C_i . The amplifier is assumed to exhibit infinite input impedance. The parallel resistance R_i should be made very high, so that its noise contribution in the passband of interest is negligible. This will be discussed in the following section on noise. Assuming that $R_i \gg \infty$, the signal current will be integrated by the input capacitance C_i , forming a voltage pulse V_i , and after passing through a suitable amplifier of very high bandwidth is then filtered by an optimum linear filter designed to optimize timing.



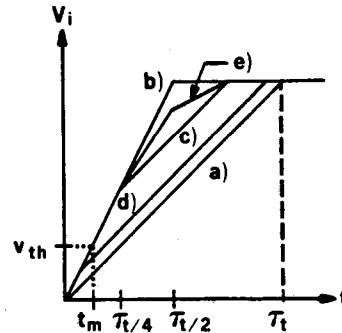
XBL 825-10004

Fig. 3. Simplified model of the timing circuit.

For the analysis a simple leading edge discriminator with a fixed threshold voltage is used to determine the timing of the pulse. In practice, the signal amplitudes vary and some form of amplitude compensation should be used, (e.g. a constant fraction discriminator). The essential limitations of the system can, however, be studied assuming a fixed signal amplitude at the input of a leading edge discriminator.

In principle, either the current or the voltage signal of the detector could be used⁴. As mentioned above, the voltage signal is formed by integrating the detector current on the input capacitance C_i . Compared to current mode operation into a 50 Ohm input impedance this may provide more than an order of magnitude improvement in signal-to-noise ratio for the detector sizes of interest in this application, even if a 'noiseless' input termination is used⁴. The reasons for this will be explained later. The following analysis will, therefore, be restricted to the voltage mode.

The voltage signals V_i for the five cases in Fig. 2 are shown in Fig. 4. Clearly, the shapes of these signals show that it is necessary to set the trigger threshold so low, that it remains in the two carrier part of the pulse transition for a sufficiently large proportion of events.



XBL 825-10008

Fig. 4. Voltage waveforms V_i corresponding to the current waveforms in Fig. 2.

Noise

The equivalent input noise sources are shown in Fig. 5. We assume that shot noise associated with the detector leakage current and the equivalent input noise current of the amplifier are negligible, a condition which is readily fulfilled. The noise source v_s accounts for the equivalent series noise resistance of the amplifier and any series resistance in the input signal path. It generates a mean square noise voltage

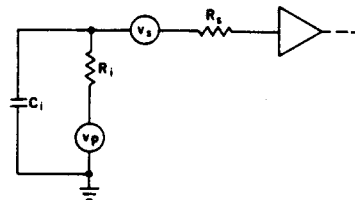
$$v_s^2 = 4kTR_s \cdot \Delta f \quad (2)$$

where Δf is the noise bandwidth of the system.

The parallel noise source v_p is primarily due to biasing networks shunting the signal input. It would also include a shunt resistor used for impedance matching. Its spectrum is attenuated at high frequencies by the input capacitance, yielding a mean square noise voltage

$$v_p^2 = \int_0^{\infty} \frac{4kTR_i}{1 + (\omega R_i C_i)^2} df \quad (3)$$

This contribution can only be neglected, if R_i is sufficiently large ($> 10^5$ Ohms in this application). A 50 Ohm matching resistor, for example, incurs a significant noise penalty.



XBL 825-10007

Fig. 5. Equivalent input noise sources.

This 'skirt' could be eliminated by using the detector current pulse for timing (i.e. choosing the input time constant $\tau_i = R_i C_i$ to be small compared to the collection time τ_c). However, resolution is severely degraded, since the additional noise incurred by the large bandwidth required for this mode outweighs the increase in slope of the signal transition. An optimum filter designed for a 1 cm thick detector operated with a 50 Ohm input resistance and $t_m = 400$ ps results in time resolution nearly seven times worse than for the voltage mode as described above. In practice the degradation will be even greater, since the average spectral noise density will be higher at the gigahertz bandwidths required. Many investigators who believe they are timing on the current pulse actually have bandwidth limitations in their systems: e.g., in the connections between the detector and the preamplifier, in subsequent amplifier stages or in the timing discriminator (Ref. 4) - which effectively integrate the signal, resulting in an inefficient form of voltage mode operation.

The curves of Fig. 8 correspond to the time resolution for a single detected energy E_d . In practice, however, the gamma-ray spectra in the Ge detector will have a range of energies and the timing spectra will therefore be a composite of individual Gaussians of different widths. In order to estimate the effective timing Gaussian width for a realistic situation, the detected energy spectrum of annihilation gamma-rays after passing through a lucite absorber of 12 cm thickness was calculated by Monte Carlo methods, providing a probability distribution $P(E)$. A Ge detector of dimensions 0.5 x 0.5 x 3 cm was assumed in the simulation. This yields the composite time response function

$$P(t) = \int_{E=200}^{511} \frac{P(E)}{\sigma \sqrt{2\pi}} \exp(-t^2/2\sigma^2) dE \quad (15)$$

where $\sigma = 3.4 \times 10^{-8}/E(\text{keV})$ for the parameters indicated above. Figure 9 shows the resulting line shape. It corresponds very closely to a Gaussian function with 240 ps FWHM, which is what would be expected for a single detected energy $E_d = 330$ keV.

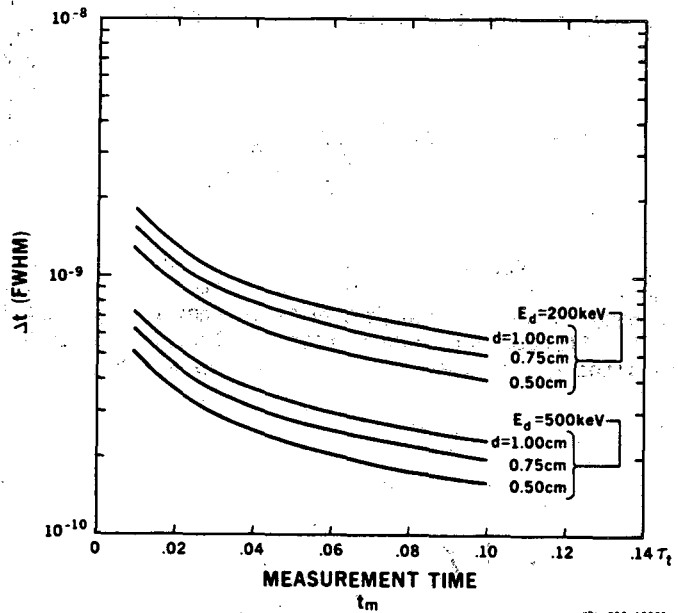


Fig. 8. Calculated time resolution FWHM as a function of the chosen measurement time t_m , for detected energies of 200 and 500 keV. The detectors are 3 cm in length, with cross sections of 0.5 x 0.5, 0.75 x 0.75 and 1.0 x 1.0 cm.

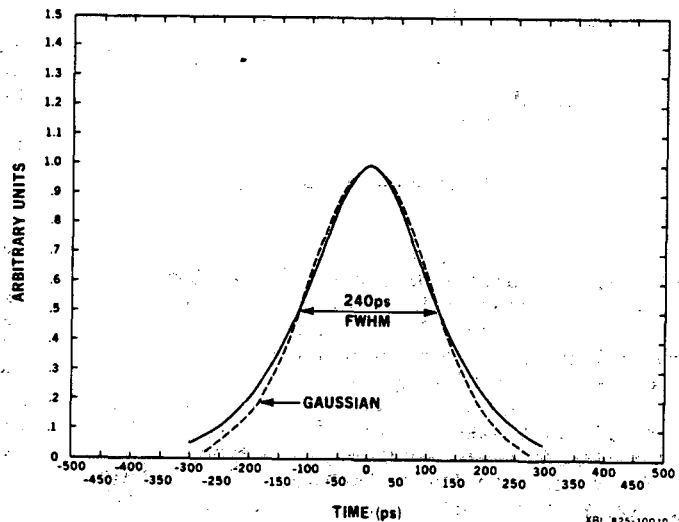


Fig. 9. Calculated timing spectrum for an energy distribution due to 511 keV gamma-rays passing through a 12 cm lucite absorber and weighted by the efficiency characteristics of the detector.

CONCLUSION

The results of this analysis show that Ge detectors offer excellent time resolution and reasonable efficiency, with overall performance quite competitive with CsF scintillation detectors. They also have additional useful features for time-of-flight positron emission tomography: small dimensions, providing reduced pixel size over scintillator arrays and a physically compact assembly, despite the requirements of vacuum and cooling.

Clearly, this analysis should be verified experimentally. In particular, considerable work is required to determine the best input amplifying device. However, the technology for fabricating large arrays of Ge detectors is well developed and we feel that this may be the right time to seriously investigate the use of germanium detectors in this promising application.

ACKNOWLEDGMENTS

We wish to acknowledge useful discussions with M. Ter-Pogossian whose friendly prodding stimulated us to pursue this investigation.

This work was prepared under the auspices of the U. S. Department of Energy Contract No. DE-AC03-76SF00098 and a grant from the National Institute of Health No. CA27024-02.

REFERENCES

1. J. Llacer and Z.H. Cho, "Preliminary Study of a Germanium Three-Dimensional Camera for Positron Emitting Radioisotopes", IEEE Trans. Nucl. Sci. NS-20, No. 1, 282-293 (1973).
2. L. Kaufman, S.H. Williams, K. Hosier, and J.H. Ewins, "An Evaluation of Semiconductor Detectors for Positron Tomography", IEEE Trans. Nucl. Sci. NS-26, No. 1, 648-653 (1979).
3. L. Kaufman, J.H. Ewins, W. Rowan, K. Hosier, M. Oberlund and D. Ortendale, "Semiconductor Gamma-Cameras in Nuclear Medicine", IEEE Trans. Nucl. Sci. NS-27, 1073 (1980).
4. H. Spieler, "Fast Timing Methods for Semiconductor Detectors", to be published in IEEE Trans. Nucl. Sci., NS-29, No. 3, (June 1982). LBL Report LBL-14145.
5. S.E. Derenzo, "Monte Carlo Calculations of the Detection Efficiency of Arrays of NaI(Tl), BGD, CsF, Ge and Plastic Detectors for 511 keV Photons", IEEE Trans. Nucl. Sci. NS-28, No. 1, 131-136 (1981).
6. V. Radeka, "Signal, Noise and Resolution in Position Sensitive Detectors", IEEE Trans. Nucl. Sci. NS-21, No. 1, 51-64 (1974).
7. J. Llacer, "Optimum Filter for Determination of the Position of an Arbitrary Waveform in the Presence of Noise", IEEE Trans. Nucl. Sci. NS-28, No. 1, 630-633 (1981).

This report was done with support from the Department of Energy. Any conclusions or opinions expressed in this report represent solely those of the author(s) and not necessarily those of The Regents of the University of California, the Lawrence Berkeley Laboratory or the Department of Energy.

Reference to a company or product name does not imply approval or recommendation of the product by the University of California or the U.S. Department of Energy to the exclusion of others that may be suitable.

TECHNICAL INFORMATION DEPARTMENT
LAWRENCE BERKELEY LABORATORY
UNIVERSITY OF CALIFORNIA
BERKELEY, CALIFORNIA 94720